Draft version December 5, 2023
Typeset using LaTeX **twocolumn** style in AASTeX631

Binary black hole mergers and intermediate-mass black holes in dense star clusters with stellar runaways

Rujuta A. Purohit [1,2] Giacomo Fragione [2,3] Frederic A. Rasio [2,3] Grayson C. Petter [1] and Ryan C. Hickox [1]

[1] Department of Physics and Astronomy, Dartmouth College, 6127 Wilder Laboratory, Hanover, NH 03755, USA
[2] Center for Interdisciplinary Exploration & Research in Astrophysics (CIERA), Northwestern University, Evanston, IL 60208, USA
[3] Department of Physics & Astronomy, Northwestern University, Evanston, IL 60208, USA

ABSTRACT

Intermediate-mass black holes (IMBHs) are believed to be the missing link between supermassive BHs that reside at the centers of massive galaxies and BHs formed as a result of stellar collapse. One of the proposed mechanisms for their formation is the stellar runaway process, where a very massive star forms from repeated stellar mergers and eventually collapses to an IMBH. In this paper, we investigate this scenario by looking at the gravitational wave (GW) events produced by this IMBH when merging with other BHs in the host star cluster. We use a state-of-the-art semi-analytic method to characterize the rates and properties of IMBH-BH mergers, as a function of the initial fraction of the initial cluster mass that collapses to from the IMBH. We also study the prospects of the detection of these mergers by current and future GW observatories, both space-based (LISA) and ground-based (LIGO's Voyager, Einstein Telescope, and Cosmic Explorer). We find that most of these merger events could be detected, with some of them being multi-band sources. Therefore, GWs represent a unique tool to test the runaway scenario and to constrain the population of IMBHs.

Keywords: Black holes – Gravitational waves – Star clusters

1. INTRODUCTION

Black holes (BHs) are observed to be abundant in the universe in two mass regimes: stellar-mass BHs formed as a result of stellar collapse, with masses $M_{\rm BH} \lesssim 100\,M_\odot$ (e.g., Celotti et al. 1999; Remillard & McClintock 2006; The LIGO Scientific Collaboration et al. 2021), and supermassive BHs found at the centers of most massive galaxies, with $M_{\rm BH} \gtrsim 10^5\,M_\odot$ (e.g., Tremaine et al. 2002; Marconi & Hunt 2003; Kormendy & Ho 2013). BHs with masses in between these two mass extremes are labeled intermediate-mass BHs (IMBHs); for a review see Greene et al. (2020). While IMBHs could play a fundamental role in the evolution of galaxies and could be a source of tidal disruption events and gravitational waves (GWs), they have not been confirmed beyond any reasonable doubt (e.g., Jardel & Gebhardt 2012; Neumayer & Walcher 2012; Graham & Scott 2013; Mezcua 2017; Nguyen et al. 2018; Perley et al. 2019; Smith et al. 2023).

IMBHs have masses beyond the most massive BH that can be originated as a result of stellar collapse. Indeed, current stellar models predict a dearth of BHs both with masses larger than about $50\,M_\odot$ as a result of pair-instability physics, where pair production removes pressure support to the star against its own collapse (Heger et al. 2003; Woosley 2017). Whenever the pre-explosion stellar core is in the range 45–65 $M_\odot$ at the onset of their carbon burning, large amounts of mass can be ejected, leaving a BH remnant with a maximum mass around $50\,M_\odot$. Larger cores can trigger thermonuclear reactions that can completely destroy the star, leaving behind no remnant.

Several mechanisms have been proposed for the formation of IMBHs. These include direct collapse of primordial gas clouds of pristine gas (e.g., Bromm & Loeb 2003; Begelman et al. 2006), the remnants of massive Population III stars in the early universe (e.g., Madau & Rees 2001; Whalen & Fryer 2012; Jiang et al. 2019), repeated mergers of main-sequence stars later collapsing

Corresponding author: Rujuta A. Purohit
rujuta.purohit.24@dartmouth.edu

into a massive BHs (e.g., Portegies Zwart & McMillan 2002; Gürkan et al. 2004; Giersz et al. 2015; Di Carlo et al. 2021; González et al. 2021), or hierarchical mergers of stellar-mass BHs (e.g., Miller & Hamilton 2002; Antonini et al. 2019; Fragione 2022).

IMBHs are primary sources for present and future GW observatories. Recent detections by the LIGO-Virgo-KAGRA (LVK) Collaboration have found binary BH (BBH) mergers where one or both components of the merging binary have masses above about $50M_\odot$. Among them, GW190521 is the most interesting event, since its remnant has a total mass of about $150M_\odot$, nominally in the IMBH regime (Abbott et al. 2020). One the main venues for the assembly of these binaries is the core of dense star clusters, where a massive BH could have resulted from the collapse of a star formed in a runaway process or hierarchical mergers (González et al. 2021; Fragione & Rasio 2023). With several hundreds detections expected in the current O4 run by the LVK Collaboration, studying BBH mergers could help us better constrain the growth and evolution of stars and BHs over time in dense clusters.

In this paper, we study a population of dense star clusters, which we assume may have hosted a runaway process that formed a very massive star (with mass $\sim 10^2 - 10^3\, M_\odot$), which ultimately resulted in an IMBH. We present simulations of merging BBHs formed in these dense clusters through a stellar runaway using the semi-analytical method developed in Fragione & Rasio (2023), and show for the first time the implications of a runaway process for GW detections by present and future observatories.

This paper is organized as follows. In Section 2, we discuss our semi-analytic method to study BH mergers in dense star clusters that host an IMBH. In Section 3, we present our results, while we summarize our study and outline future work in Section 4.

2. METHODS

In this Section, we include a summary of the semi-analytical method we use to derive our results. For a detailed discussion, see § 2 of Fragione & Rasio (2023).

We consider a dense stellar cluster of initial mass $M_{\rm CL}$, in the range $[10^5 M_\odot,\, 10^7 M_\odot]$, and half-mass–radius $r_{\rm h} = 1\,{\rm pc}$. We sample stellar masses from the canonical Kroupa initial mass function (Kroupa 2001):

$$\xi(m_\star) \propto \begin{cases} \left(\frac{m_\star}{0.5 M_\odot}\right)^{-1.3} & \text{if } 0.08 \le \frac{m_\star}{M_\odot} \le 0.50 \\ \left(\frac{m_\star}{0.5 M_\odot}\right)^{-2.3} & \text{if } 0.50 \le \frac{m_\star}{M_\odot} \le 150\,. \end{cases} \quad (1)$$

Given this IMF, we sample a total of

$$N_{\rm BH} = 3.025 \times 10^3 \left(\frac{M_{\rm CL}}{10^6 M_\odot}\right) \quad (2)$$

BH progenitors, in the mass range $[20M_\odot,\, 150M_\odot]$. We consider cluster metallicities $Z \in \{0.02, 0.002, 0.0002\}\ Z_\odot$, and evolve the BH progenitors at a given metallicity using SSE Hurley et al. (2000), with all the necessary updated prescriptions for stellar winds, stellar interactions, and formation of remnants (for details see Banerjee et al. 2020). After formation, each BH is imparted a natal kick sampled from a Maxwellian distribution with velocity dispersion $265\,{\rm km\,s^{-1}}$ (Hobbs et al. 2005), scaled by a factor of $1.4\,M_\odot$ to account for momentum conservation (Fryer & Kalogera 2001). If the GW recoil kick exceeds the cluster escape velocity,

$$v_{\rm esc} = 32\,{\rm km\,s^{-1}} \left(\frac{M_{\rm CL}}{10^5\,M_\odot}\right)^{1/2} \left(\frac{r_{\rm h}}{1\,{\rm pc}}\right)^{-1/2}\,, \quad (3)$$

the BH is ejected from the cluster. Finally, we assume that all BHs are born with negligible natal spins, consistent with Fuller & Ma (2019).

In our simulation, we model cluster evolution by following Antonini & Gieles (2020a,b). Briefly, the cluster is assumed to reach a state of balanced evolution, so that the heat generated by the BBHs in the core and the cluster global properties are related. Our simulations include all the fundamental elements of cluster evolution (cluster mass loss and expansion) and the fundamental processes of formation and evolution of BBHs (3-body interactions, mergers, recoil kicks, etc.). In Fragione & Rasio (2023), it was shown that this semi-analytical method performs well at reproducing the essential elements of BBH mergers, especially when compared to N-body simulations. For more details, see Antonini & Gieles (2020a,b) and Fragione & Rasio (2023).

In our study, we add a novel parameter compared to the scheme presented in Fragione & Rasio (2023), $f_{\rm run}$, which represents the fraction of cluster mass that undergoes a runaway process. The mass of the star formed as a result of the runaway is

$$m_{\rm run} = f_{\rm run}\, M_{\rm CL}. \quad (4)$$

Note that we assume that every cluster goes through a runaway process regardless of its initial mass and density. Even if this may not be the case for real clusters and other parameters (slope of the initial mass function, primordial binary fraction in massive stars, etc.) could play a role (e.g., González et al. 2021), we leave their detailed exploration to an upcoming paper.

In our simulations, we consider four different cases, with $f_{\rm run} \in \{0, 0.0005, 0.001, 0.005, 0.01\}$. For each value of $f_{\rm run}$, we run 5000 simulations for each metallicity. The clusters have masses in the range $M_{\rm CL} \in [10^5, 10^7]$ assuming a distribution of cluster masses $\propto M_{\rm CL}^{-2}$ (Portegies Zwart et al. 2010). The half-mass radius is fixed at $r_{\rm h} = 1\,$pc, representative of the typical size of young massive clusters (Portegies Zwart et al. 2010).

3. RESULTS

In this Section, we summarize the results of our simulations and discuss the detectability of the BBH mergers by present and upcoming GW observatories.

3.1. *Growth of an IMBH*

In our simulations, we started our star clusters with a massive IMBH, remnant of the collapse of a large star resulting from the runaway process (e.g., Portegies Zwart & McMillan 2002; González et al. 2021). This IMBH may grow through repeated mergers with other BHs over time, whenever not ejected as a consequence of dynamical kicks in few-body interactions or recoil kicks after a merger via GW emission. We track the growth of the most massive BH in each cluster as a result of repeated mergers with other stellar BHs.

In Figure 1, we show the most massive BH formed in a star cluster as a function of the initial cluster mass for various values of the fraction of cluster mass that undergoes a runaway process. As expected, a larger value of $f_{\rm run}$ implies a larger most massive BH across all initial cluster masses. For example, we find that a cluster of initial mass of $10^5\,M_\odot$, $f_{\rm run}=0$ leads to a most massive BH of about $80 M_\odot$, $f_{\rm run}=0.001$ of about $1.1\times10^3 M_\odot$, and $f_{\rm run}=0.01$ of about $4.5\times10^3 M_\odot$.

The value of $f_{\rm run}$ is particularly crucial for small clusters. In particular, this is because for smaller values of $f_{\rm run}$ the smaller IMBHs are ejected from the cluster due to dynamical or recoil kicks after the mergers. For example, in the case there is no runaway ($f_{\rm run}=0$), clusters with masses $\lesssim 10^6\,M_\odot$ do not form an IMBH; however, the most massive IMBH for a cluster of mass $\sim 10^6 M_\odot$ has a mass of about $5\times10^3 M_\odot$ for $f_{\rm run}=0.001$, while a mass of about $3\times10^4 M_\odot$ for $f_{\rm run}=0.01$.

To provide additional insight into the formation of massive black holes within clusters, Figure 2 illustrates the fractional number of clusters, or *likelihood*, of the most massive BH surpassing a specified mass threshold in our simulations. When $f_{\rm run}=0$ (no runaway effect), only very massive clusters exhibit a non-negligible probability of hosting massive BHs. Conversely, with higher $f_{\rm run}$ values, the runaway IMBH initial mass is inherently substantial, increasing the likelihood of finding them even in less massive clusters, as ejections become less important.

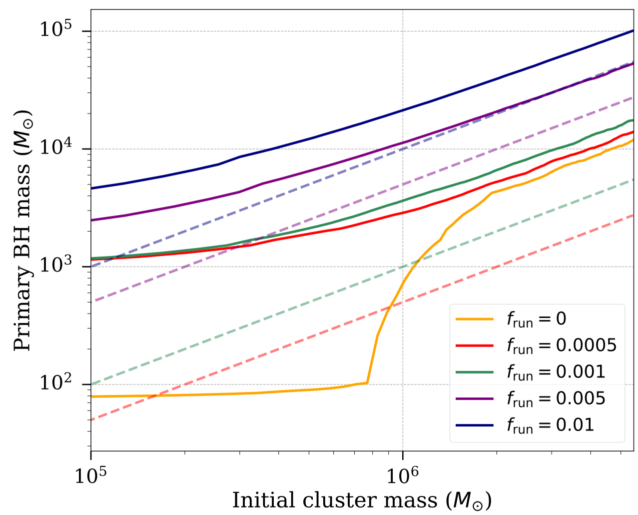

Figure 1. Solid lines: most massive BH formed in a cluster as a function of the initial cluster mass for different values of the fraction of cluster mass that undergoes a runaway process, $f_{\rm run}$. The half-mass radius is fixed at $r_{\rm h} = 1\,$pc representative of the typical size of young massive clusters. Dashed lines: initial IMBH mass, $m_{\rm run} = f_{\rm run} M_{\rm CL}$, as a function of the initial cluster mass.

3.2. *BBH merger rates*

We follow Fragione & Rasio (2023) and calculate the rates (in units of Gpc^{-3} yr^{-1}) of BBH mergers as[1]

$$R(z) = K \frac{d}{dt_{\rm lb}} \int\int\int\int dM_{\rm CL}\, dr_h\, dZ\, dz_f \frac{dt_{\rm lb}}{dz_f} \times \frac{\partial N_{\rm events}}{\partial M_{\rm CL}\, \partial r_h\, \partial Z\, \partial z_f} \Psi(M_{\rm CL} r_h, Z, z_f)\,, \tag{5}$$

where $t_{\rm lb}$ is the look-back time at redshift z, $N_{\rm events}$ is the number of events as a function of the initial cluster mass $M_{\rm CL}$, initial half-mass radius $r_{\rm h}$, metallicity Z, and formation redshift $z_{\rm f}$, and $\Psi(M_{\rm CL}, r_h, Z, z_f)$ is a probability function that weighs the the previous cluster properties. In our model, we take the distribution of cluster masses to be $\propto M_{\rm CL}^{-2}$, with the maximum possible cluster mass being $M_{\rm CL}= 10^7 M_\odot$ (e.g., Portegies Zwart & McMillan 2000). We fix the half-mass radius to $r_{\rm h} = 1\,$pc, which follows the typical distribution for of observed values for local, young stellar clusters (Portegies Zwart et al. 2010). Following Mapelli et al. (2021), we take the formation times to be proportional to $\exp[-(z - z_f)^2/(2\sigma_f^2)]$ where $z_f = 3.2$ and $\sigma_f = 1.5$,

[1] In this work, we adopt a standard ΛCDM cosmology (Planck Collaboration et al. 2016): $H_0 = 67.8$ km s^{-1} Mpc^{-1}, $\Omega_{\rm m} = 0.308$, and $\Omega_\Lambda = 0.692$.

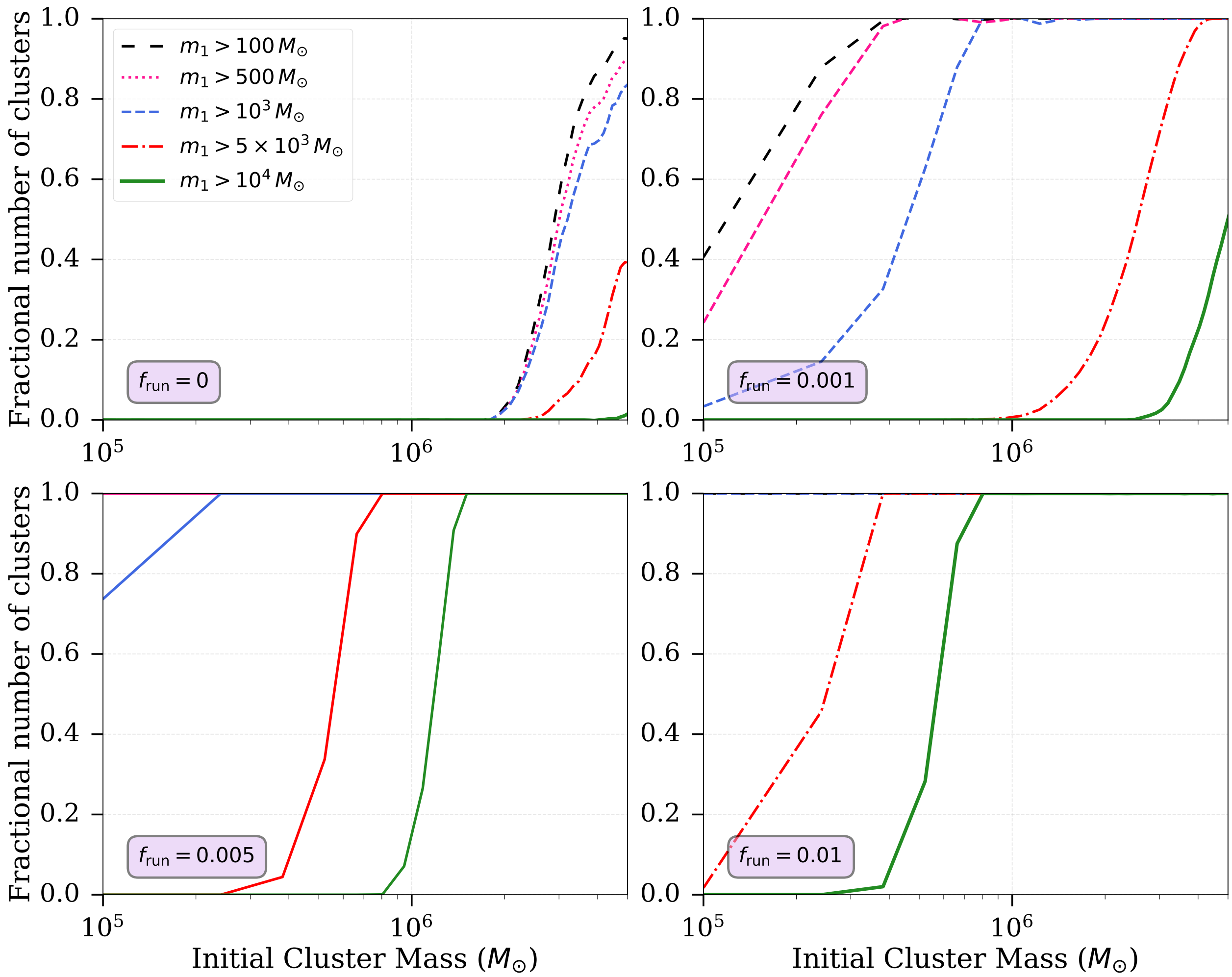

Figure 2. The fractional number of clusters that develop a massive BH as a function of the initial cluster mass. For a larger fraction of runaway rate, the number of clusters with massive BHs increases for lower cluster mass. We show 5 different mass thresholds: 100, 500, 10^3, 5×10^3, $10^4 M_\odot$.

reminiscent of cluster formation times as inferred from cosmological simulations. Metallicities are sampled from a log-normal distribution with mean given by (Madau & Fragos 2017)

$$\log\langle Z/\mathrm{Z}_\odot\rangle = 0.153 - 0.074\,z^{1.34} \tag{6}$$

and a standard deviation of 0.5 dex. In Equation 5, K accounts for the cluster density evolution, considering that a fraction of the star clusters that are formed in the universe evaporate across cosmic time. We fix $K = 32.5$, consistent with Antonini & Gieles (2020a) and with the value needed to reproduce the merger rates of BBH mergers in the latest LVK catalog (Fishbach & Fragione 2023).

We calculate the BBH merger rate as a function of redshift for each values of the runaway fraction. Figure 3 shows the overall merger rate for our models, which we also break down to show the contribution of IMBH of different masses $(100, 200, 500, 1000\,M_\odot)$. We find that relative contribution of massive BHs is larger for larger values of $f_{\rm run}$, since the IMBH starts dominating the merger rate, as it keeps merging repeatedly with the other stellar-mass BHs. Indeed, we find that $f_{\rm run}=0$ has a merger rate of 19 Gpc^{-3} yr^{-1}, $f_{\rm run}=0.001$ of 6.2 Gpc^{-3} yr^{-1}, $f_{\rm run}=0.005$ of 2.9 Gpc^{-3} yr^{-1}, and $f_{\rm run}=0.01$ of 2.24 Gpc^{-3} yr^{-1}. At the same time, the merger rate for primary masses larger than $1000 M_\odot$ for $f_{\rm run}=0$ is of 0.09 Gpc^{-3} yr^{-1}, for $f_{\rm run}=0.001$ of 1.66 Gpc^{-3} yr^{-1}, for $f_{\rm run}=0.005$ of 2.03 Gpc^{-3} yr^{-1}, and for $f_{\rm run}=0.01$ of 2.24 Gpc^{-3} yr^{-1}.

3.3. *Detectability of merging BBH with GW instruments*

It is critical to understand whether, given a population of merging BBHs, current and upcoming ground-based and space-based instruments are likely or not

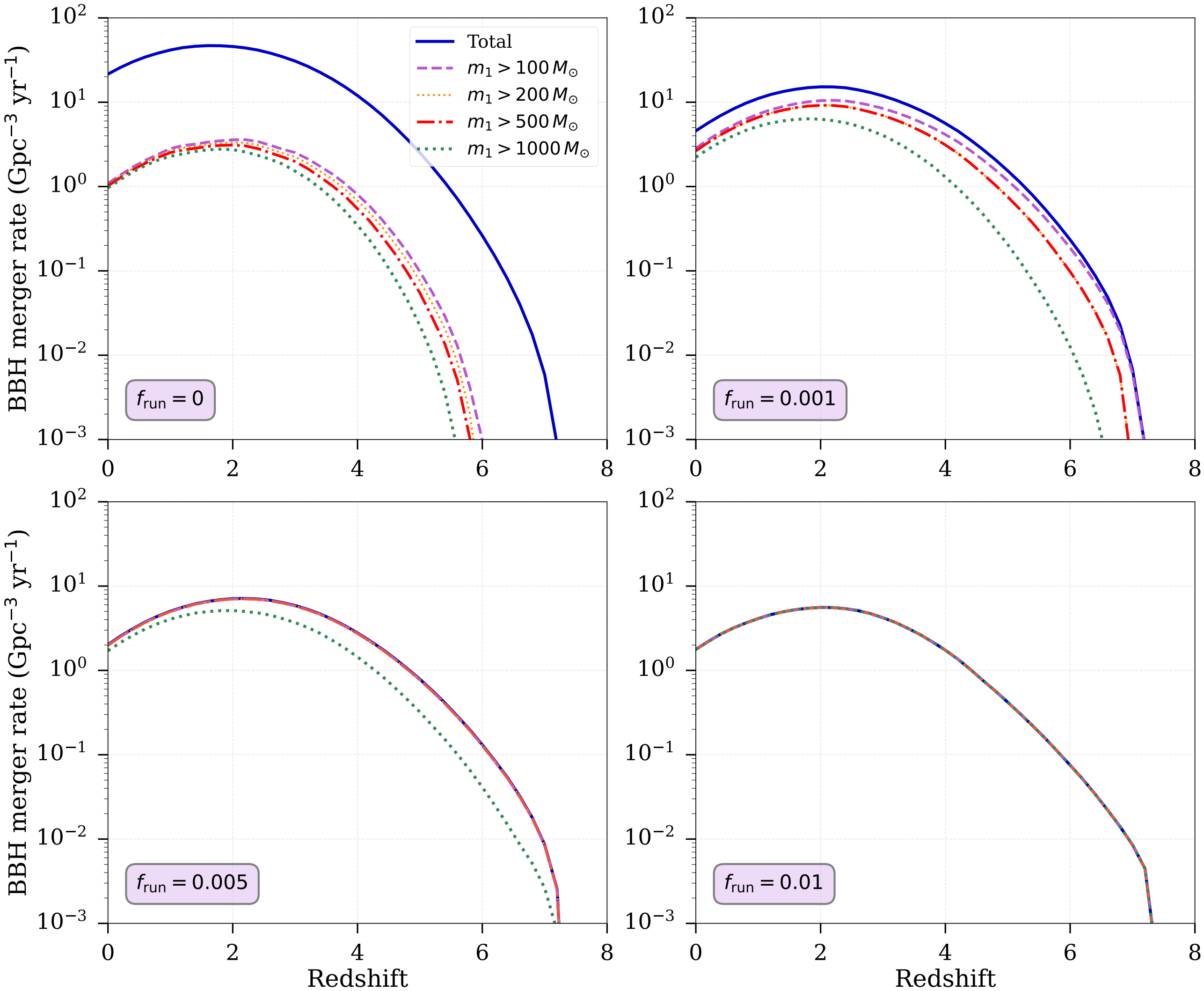

Figure 3. The binary black hole (BBH) merger rate as a function of redshift for four different fractions of initial cluster mass that undergo the stellar runaway. The total merger rate is shown, along with rates for a primary mass over a given threshold for the primary mass: $100, 200, 500, 1000 M_\odot$.

to detect a fraction of them. We calculate the detection fraction of these merger events for planned ground- and space-based GW instruments, such as Laser Interferometer Space Antenna (LISA; Robson et al. 2019), Voyager (the upgraded detector of the current LIGO facility The LIGO Scientific collaboration 2019), the Einstein Telescope (ET; Punturo et al. 2010), and the Cosmic Explorer (CE; Reitze et al. 2019). While LIGO/Virgo/KAGRA could detect the mergers of BBHs with masses final $\sim 100 M_\odot$ out to redshifts of $z \sim 1$ (Abbott et al. 2019), the upcoming space-based LISA and ground-based instruments like ET and CE offer the opportunity of detecting IMBHs up to $z \sim 10-100$ (Amaro-Seoane et al. 2017; Jani et al. 2020; Fragione & Loeb 2023). Thus, understanding the probability of actual detection of these events would guide our search for BBH systems and help plan future observing cycles.

We follow Fragione & Loeb (2023) and use the detection fraction as an instrument-dependent function, which encodes the ability of observing the merger of a binary with primary mass m_1 and mass ratio q at a redshift z. The masses and merger times are obtained directly form our simulations. However, the merger times need to be corrected for the cluster formation time. As for the merger rates, we take the formation times to be proportional to $\exp[-(z-z_f)^2/(2\sigma_f^2)]$ where $z_f = 3.2$ and $\sigma_f = 1.5$, reminiscent of cluster formation times as inferred from cosmological simulations. Once we correct for the cluster formation, we discard those binaries that have a merger time larger than the age of the universe.

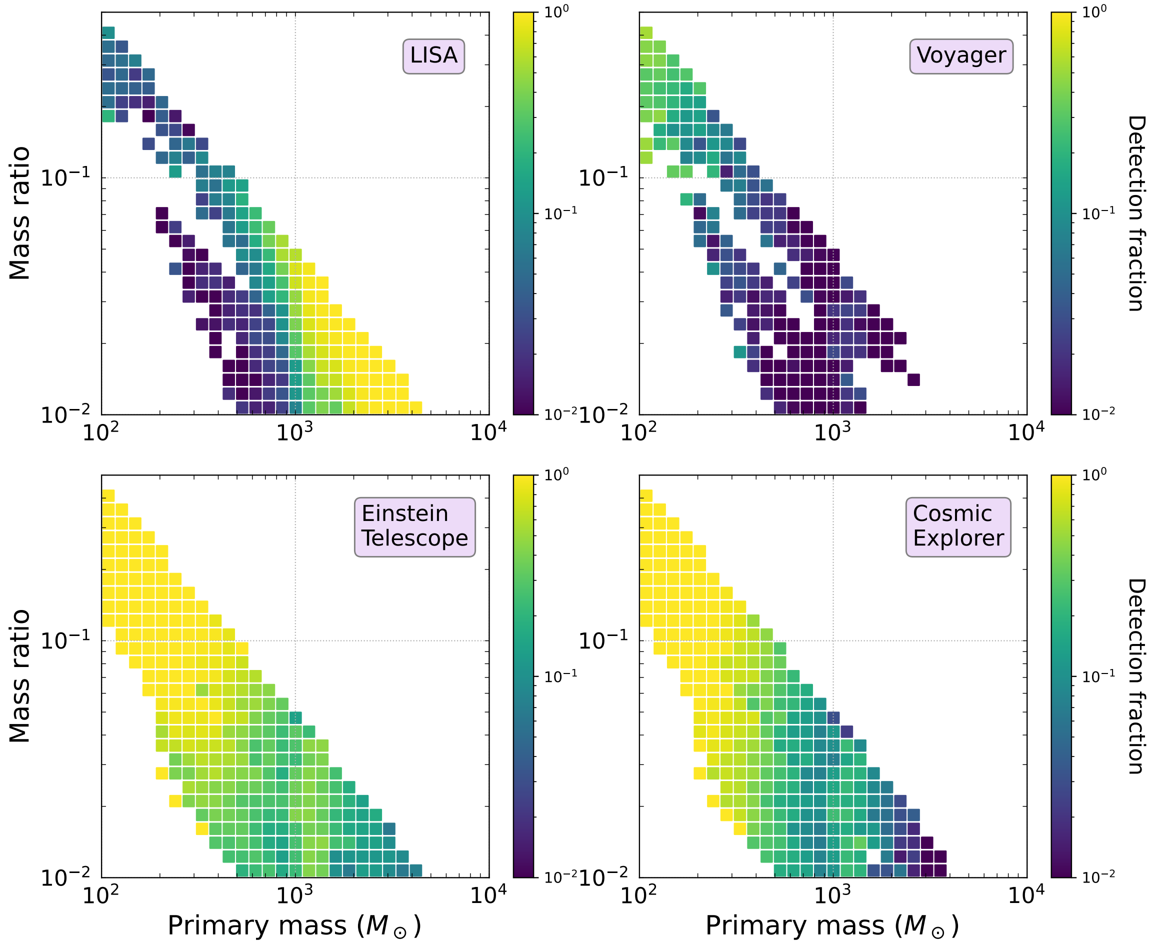

Figure 4. The detection fraction for merging IMBH binaries as a function of the primary mass and mass ratio in clusters with stellar runaways. This figure shows the detection fraction for merger events in clusters with $f_{\rm run}$= 0.001. Top left: LISA; top right: Voyager; bottom left: Einstein Telescope; bottom right: Cosmic Explorer.

The sources not discarded are kept in our data and their merger times are converted to redshift.

The detection of a merger event is modeled as an instrument-dependent function $F_{\rm det}(z, m_1, q)$ as

$$F_{\rm det}(z, m_1, q) = H(\langle\rho(z, m_1, q)\rangle > \rho_{\rm thresh})\,, \qquad (7)$$

where H is the Heaviside function and $\langle\rho(z, m_1, q)\rangle$ is the averaged signal-to-noise (SNR) ratio. The threshold for a detection is set to an SNR of 8. From Fragione & Loeb (2023), we compute the average SNR as

$$\langle\rho(z, m_1, q)\rangle = 2C\sqrt{\int_{f_{\rm min}}^{f_{\rm max}} \frac{|\tilde{h}f|^2}{S_n(f)}df}\,, \qquad (8)$$

where C is obtained after averaging over various sky relations, with $C = 2/\sqrt{5}$ and $C = 2/5$ for space-based and ground-based detectors, respectively (Robson et al. 2019); $f_{\rm min}$ and $f_{\rm max}$ are the minimum and maximum frequency of the binary in the detector band, respectively; $S_{\rm n}(f)$ is the noise power spectral density; $|\tilde{h}(f)|$ is the frequency-domain waveform amplitude for a face-on binary. We use pyCBC developed by Nitz et al. (2019) with the IMRPhenomD approximant (Husa et al. 2016) to model the waveform of the merging binary BHs.

We study the detection probability of these merger events using four different gravitational wave observatories: space-based LISA and ground-based Voyager, ET, and CE. The power spectral density of LISA is derived as in Robson et al. (2019), of Voyager as in The LIGO Scientific collaboration (2019), of ET as in Punturo et al. (2010), and of CE as in Reitze et al. (2019). Note that the space-based mission LISA has a planned duration of 5 years, and a binary will evolve towards a merger event as it starts from the frequency

$$f_{\rm ini} = 1.2\times10^{-2}\,{\rm Hz}\,(1+{\rm z})^{-\frac{5}{8}}\left(\frac{1+{\rm q}}{{\rm q}^3}\right)^{\frac{1}{8}} \times\left(\frac{m_1}{100M_\odot}\right)^{-\frac{5}{8}}\left(\frac{T_{\rm LISA}}{4{\rm yr}}\right)^{-\frac{3}{8}}. \qquad (9)$$

This initial frequency is higher than the minimum detectable frequency for LISA which is conventionally 10^{-5} Hz. Thus, we take, $f_{\rm min} = f_{\rm ini}$ for LISA. For the ground-based instruments in the study namely Voyager, ET, and CE, this initial frequency $f_{\rm ini}$ is typically smaller than the frequency at which the instruments start operating, 5 Hz, 1 Hz, and 5 Hz, respectively.

In Figure 4, we show the detection probability of BBH merger events in clusters, with $f_{\rm run}$= 0.001. We see that LISA is able to detect most of the mergers with primary mass $\gtrsim 10^3 M_\odot$ and mass ratio $10^{-2} \lesssim q \lesssim 10^{-1}$. For the smaller masses, LISA is only able to detect a few of the merging IMBH binaries. Conversely, the population of merging binaries with $m_1 \lesssim 10^3 M_\odot$ can be studied using ground-based instruments. LIGO's Voyager is only able to detect a few of the merging binaries in this regime, in particular when the mass ratio is not too far from unity. ET and CE are able to detect most binaries with primary mass $m_1 \lesssim 10^3 M_\odot$ and mass ratio $\sim 10^{-1}$.

The plots showing detection fractions for other values of $f_{\rm run}$ are included in the Appendix.

4. CONCLUSION AND DISCUSSION

In this paper, we analyzed simulations of merging BBHs in dense clusters, where an IMBH is assumed to be formed as result of the collapse of a massive star created from repeated stellar mergers. Here, we summarize our main findings:

- The presence of an IMBH born as the remnant of stellar runaways grows in time through repeated mergers with stellar-mass BHs, up to about 2-3 times its initial mass.
- With stellar runaways, star clusters may originate IMBHs of masses $\sim 10^2$-$10^3\, M_\odot$, which further grow to $\gtrsim 10^3 M_\odot$ through repeated mergers with other stellar-mass BHs. This is not seen for the case $f_{\rm run}$= 0 when BHs grow solely through mergers in clusters of all sizes.
- The merger rate of BBHs dynamically assembled in dense star clusters tends to become smaller if the mass of the IMBH formed as a result of a runaway process is larger. For sufficiently large masses, the IMBH dominates the merger rate and the number of mergers of stellar-mass BHs are negligible.
- The merging binary systems that LISA can potentially detect map the underlying astrophysical population for with primary masses $m_1 > 100\, M_\odot$ and mass ratio $1 > q > 10^{-2}$. The ground-based instruments ET and CE will be capable to observe the lower-mass binaries, with primary mass $m_1 < 10^3 M_\odot$ and mass ratio $q > 10^{-2}$, while the detection efficiency of Voyager is typically very small.

While our models represent a significant improvement upon previous literature, there are some caveats that we leave to future work. For example, we have not included in our treatment the interaction of the IMBH with stars, which could lead to interesting phenomena, such as tidal events (e.g., Liu et al. 2009; Fragione et al. 2021; Angus et al. 2022). We have also fixed some of the distributions that describe the birth properties of star clusters, consistent with observed properties in the local universe (Portegies Zwart et al. 2010), but these are poorly constrained. Furthermore, we have used the IMRPhenomD as our approximation for the waveform, which only includes the dominant harmonic $(l, m) = (2, 2)$ of the GW signal. However, higher order harmonics could contribute to the GW signal significantly, especially for IMBH binaries (Jani et al. 2020). Finally, another important yet currently uncertain point question is the fate of the very massive star (with mass $\sim 10^2 - 10^3\, M_\odot$) that is produced as result of the runaway process, as stellar evolutionary models have not been calibrated over that mass range. As Mapelli (2016) notes, the mass of the final remnant is in the IMBH mass range only if mass-loss by stellar winds is moderate and only if it a direct collapse into a BH takes place.

GWs offer an unparalleled opportunity to survey the sky and detect IMBHs, making it possible for the first time to constrain their formation, growth, and merger history across cosmic time.

APPENDIX

Here, we include the plots for the detection fractions, similarly to Figure 7, for values of $f_{\rm run}$= 0, 0.001 and 0.005.

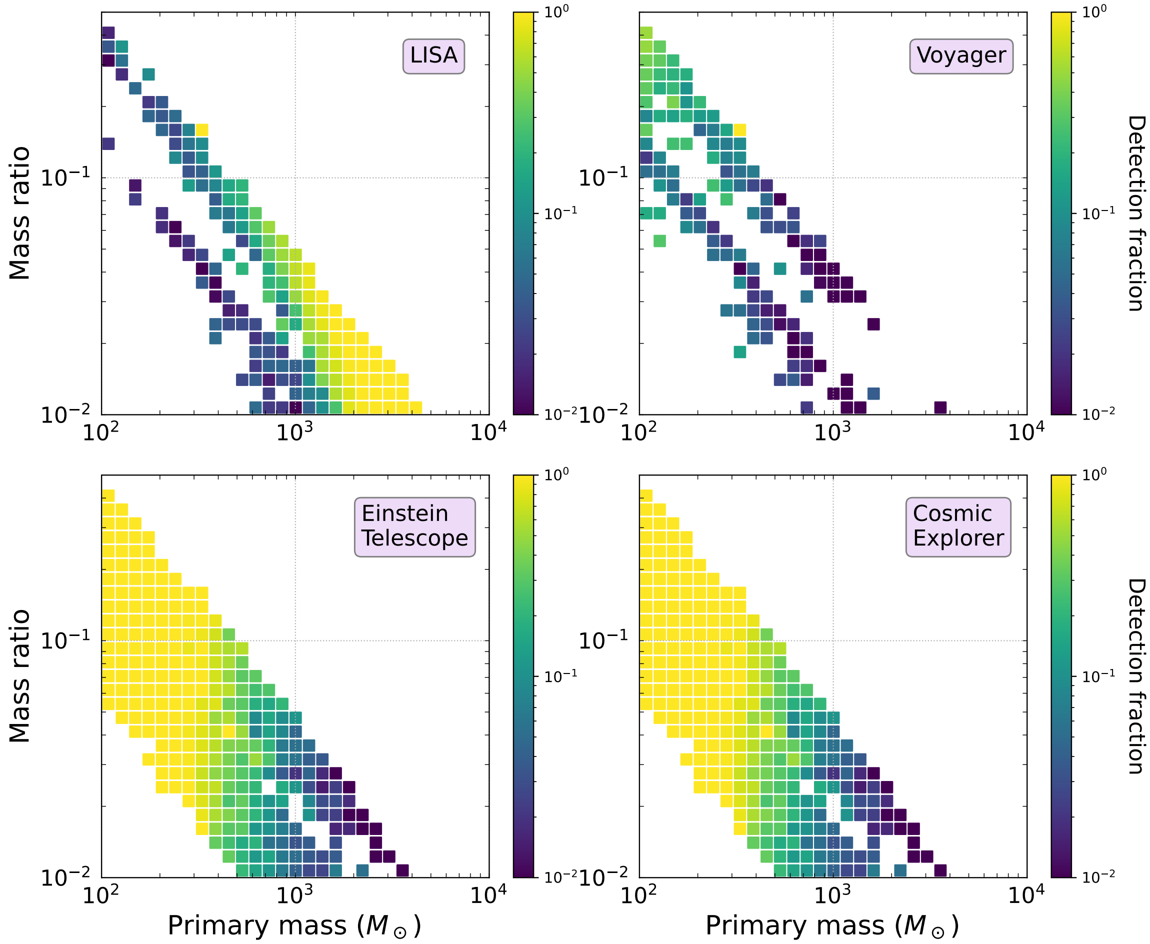

Figure 5. Same as Figure 7 but for $f_{\rm run}$= 0.

R.A.P acknowledges support from the Student Experiential Learning Fund and the Undergraduate Advising and Research at Dartmouth College. This work was supported by NASA Grant 80NSSC21K1722 and NSF Grant AST-2108624 at Northwestern University (to G.F. and F.A.R.). R.A.P was a summer student at the CIERA REU directed by Dr Aaron Geller. This research was supported in part through the computational resources and staff contributions provided for the Quest high performance computing facility at Northwestern University which is jointly supported by the Office of the Provost, the Office for Research, and Northwestern University Information Technology. This material is based upon work supported by the National Science Foundation under grant No. AST 2149425, a Research Experiences for Undergraduates (REU) grant awarded to CIERA at Northwestern University. Any opinions, findings, and conclusions or recommendations expressed in this material are those of the author(s) and do not necessarily reflect the views of the National Science Foundation.

Software: `scipy` (Virtanen et al. 2020), `astropy` (Astropy Collaboration et al. 2018), `imbhistory` (Fragione 2023)

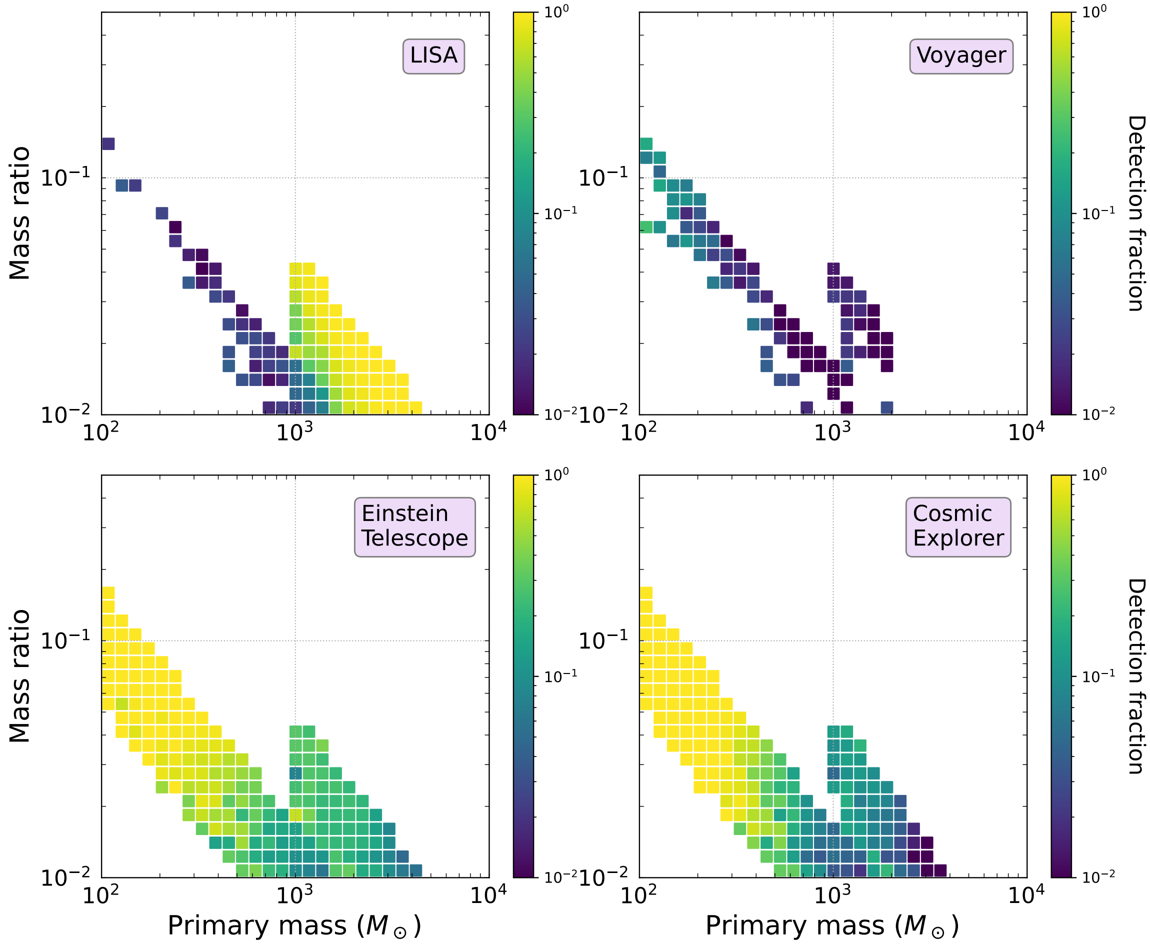

Figure 6. Same as Figure 4 but for $f_{\rm run}$= 0.005.

REFERENCES

Abbott, B. P., Abbott, R., Abbott, T. D., et al. 2019, PhRvD, 100, 064064, doi: 10.1103/PhysRevD.100.064064

Abbott, R., Abbott, T. D., Abraham, S., et al. 2020, PhRvL, 125, 101102, doi: 10.1103/PhysRevLett.125.101102

Amaro-Seoane, P., Audley, H., Babak, S., et al. 2017, arXiv e-prints, arXiv:1702.00786, doi: 10.48550/arXiv.1702.00786

Angus, C. R., Baldassare, V. F., Mockler, B., et al. 2022, Nature Astronomy, 6, 1452, doi: 10.1038/s41550-022-01811-y

Antonini, F., & Gieles, M. 2020a, PhRvD, 102, 123016, doi: 10.1103/PhysRevD.102.123016

—. 2020b, MNRAS, 492, 2936, doi: 10.1093/mnras/stz3584

Antonini, F., Gieles, M., & Gualandris, A. 2019, MNRAS, 486, 5008, doi: 10.1093/mnras/stz1149

Astropy Collaboration, Price-Whelan, A. M., Sipőcz, B. M., et al. 2018, AJ, 156, 123, doi: 10.3847/1538-3881/aabc4f

Banerjee, S., Belczynski, K., Fryer, C. L., et al. 2020, A&A, 639, A41, doi: 10.1051/0004-6361/201935332

Begelman, M. C., Volonteri, M., & Rees, M. J. 2006, MNRAS, 370, 289, doi: 10.1111/j.1365-2966.2006.10467.x

Bromm, V., & Loeb, A. 2003, ApJ, 596, 34, doi: 10.1086/377529

Celotti, A., Miller, J. C., & Sciama, D. W. 1999, Classical and Quantum Gravity, 16, A3, doi: 10.1088/0264-9381/16/12A/301

Di Carlo, U. N., Mapelli, M., Pasquato, M., et al. 2021, MNRAS, 507, 5132, doi: 10.1093/mnras/stab2390

Fishbach, M., & Fragione, G. 2023, MNRAS, 522, 5546, doi: 10.1093/mnras/stad1364

Fragione, G. 2022, ApJ, 939, 97, doi: 10.3847/1538-4357/ac98b6

—. 2023, giacomofragione/imbhistory: imbhistory v1.01, v1.01, Zenodo, Zenodo, doi: 10.5281/zenodo.7530024

Fragione, G., & Loeb, A. 2023, ApJ, 944, 81, doi: 10.3847/1538-4357/acb34e

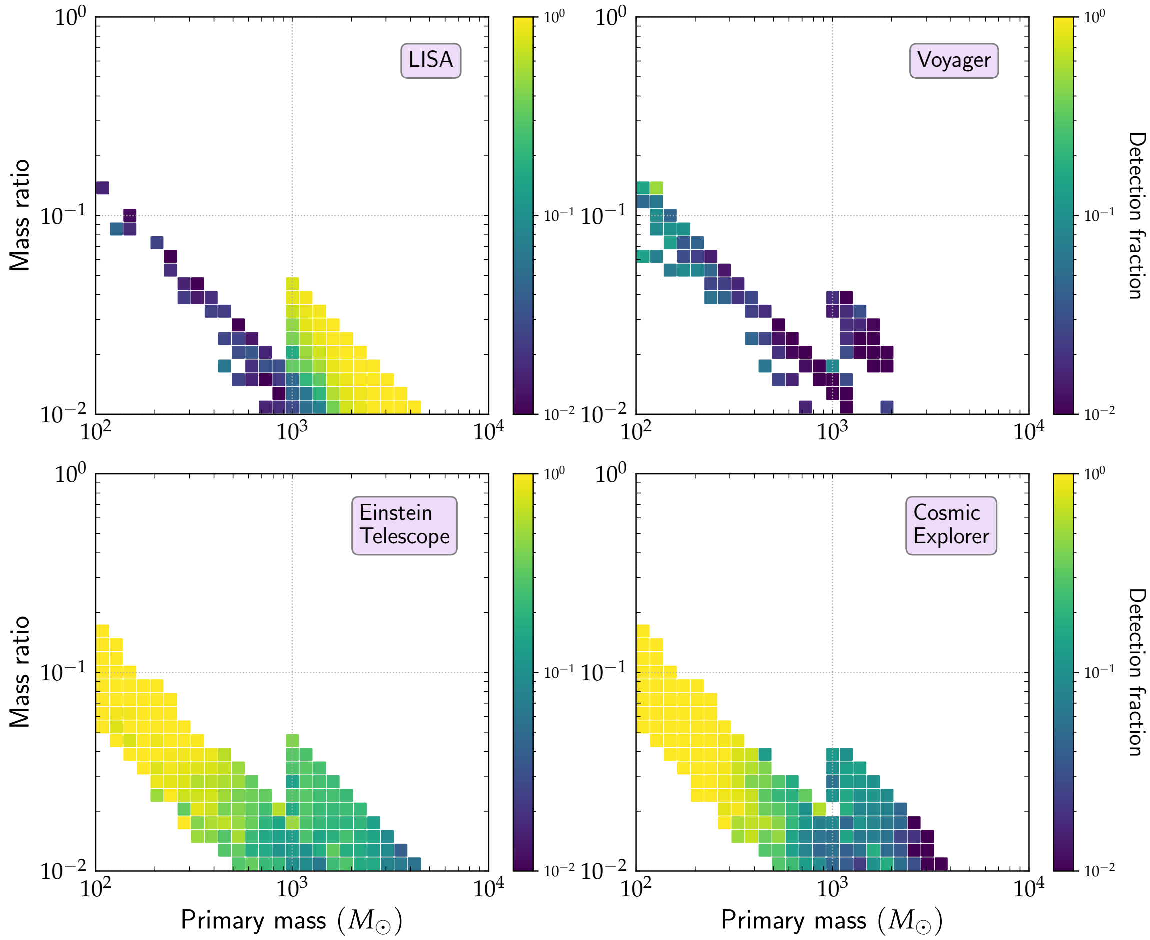

Figure 7. Same as Figure 4 but for $f_{\rm run}$= 0.01.

Fragione, G., Perna, R., & Loeb, A. 2021, MNRAS, 500, 4307, doi: 10.1093/mnras/staa3493

Fragione, G., & Rasio, F. A. 2023, ApJ, 951, 129, doi: 10.3847/1538-4357/acd9c9

Fryer, C. L., & Kalogera, V. 2001, ApJ, 554, 548, doi: 10.1086/321359

Fuller, J., & Ma, L. 2019, ApJL, 881, L1, doi: 10.3847/2041-8213/ab339b

Giersz, M., Leigh, N., Hypki, A., Lützgendorf, N., & et al. 2015, MNRAS, 454, 3150, doi: 10.1093/mnras/stv2162

González, E., Kremer, K., Chatterjee, S., et al. 2021, ApJL, 908, L29, doi: 10.3847/2041-8213/abdf5b

Graham, A. W., & Scott, N. 2013, ApJ, 764, 151, doi: 10.1088/0004-637X/764/2/151

Greene, J. E., Strader, J., & Ho, L. C. 2020, ARA&A, 58, 257, doi: 10.1146/annurev-astro-032620-021835

Gürkan, M. A., Freitag, M., & Rasio, F. A. 2004, ApJ, 604, 632, doi: 10.1086/381968

Heger, A., Fryer, C. L., Woosley, S. E., Langer, N., & Hartmann, D. H. 2003, ApJ, 591, 288, doi: 10.1086/375341

Hobbs, G., Lorimer, D. R., Lyne, A. G., & Kramer, M. 2005, MNRAS, 360, 974, doi: 10.1111/j.1365-2966.2005.09087.x

Hurley, J. R., Pols, O. R., & Tout, C. A. 2000, MNRAS, 315, 543, doi: 10.1046/j.1365-8711.2000.03426.x

Husa, S., Khan, S., Hannam, M., et al. 2016, PhRvD, 93, 044006, doi: 10.1103/PhysRevD.93.044006

Jani, K., Shoemaker, D., & Cutler, C. 2020, Nature Astronomy, 4, 260, doi: 10.1038/s41550-019-0932-7

Jardel, J. R., & Gebhardt, K. 2012, ApJ, 746, 89, doi: 10.1088/0004-637X/746/1/89

Jiang, Y.-F., Stone, J. M., & Davis, S. W. 2019, ApJ, 880, 67, doi: 10.3847/1538-4357/ab29ff

Kormendy, J., & Ho, L. C. 2013, ARA&A, 51, 511, doi: 10.1146/annurev-astro-082708-101811

Kroupa, P. 2001, MNRAS, 322, 231, doi: 10.1046/j.1365-8711.2001.04022.x

Liu, F. K., Li, S., & Chen, X. 2009, ApJL, 706, L133, doi: 10.1088/0004-637X/706/1/L133

Madau, P., & Fragos, T. 2017, ApJ, 840, 39, doi: 10.3847/1538-4357/aa6af9

Madau, P., & Rees, M. J. 2001, ApJL, 551, L27, doi: 10.1086/319848

Mapelli, M. 2016, MNRAS, 459, 3432, doi: 10.1093/mnras/stw869

Mapelli, M., Dall'Amico, M., Bouffanais, Y., et al. 2021, MNRAS, 505, 339, doi: 10.1093/mnras/stab1334

Marconi, A., & Hunt, L. K. 2003, ApJL, 589, L21, doi: 10.1086/375804

Mezcua, M. 2017, International Journal of Modern Physics D, 26, 1730021, doi: 10.1142/S021827181730021X

Miller, M. C., & Hamilton, D. P. 2002, MNRAS, 330, 232, doi: 10.1046/j.1365-8711.2002.05112.x

Neumayer, N., & Walcher, C. J. 2012, Advances in Astronomy, 2012, 709038, doi: 10.1155/2012/709038

Nguyen, D. D., Seth, A. C., Neumayer, N., et al. 2018, ApJ, 858, 118, doi: 10.3847/1538-4357/aabe28

Nitz, A., Harry, I., Brown, D., et al. 2019, gwastro/pycbc: PyCBC Release v1.15.2, v1.15.2, Zenodo, Zenodo, doi: 10.5281/zenodo.3564824

Perley, D. A., Mazzali, P. A., Yan, L., Cenko, S. B., & et al. 2019, MNRAS, 484, 1031, doi: 10.1093/mnras/sty3420

Planck Collaboration, Ade, P. A. R., Aghanim, N., et al. 2016, A&A, 594, A13, doi: 10.1051/0004-6361/201525830

Portegies Zwart, S. F., & McMillan, S. L. W. 2000, ApJL, 528, L17, doi: 10.1086/312422

—. 2002, ApJ, 576, 899, doi: 10.1086/341798

Portegies Zwart, S. F., McMillan, S. L. W., & Gieles, M. 2010, ARA&A, 48, 431, doi: 10.1146/annurev-astro-081309-130834

Punturo, M., Abernathy, M., Acernese, F., et al. 2010, Classical and Quantum Gravity, 27, 194002, doi: 10.1088/0264-9381/27/19/194002

Reitze, D., Adhikari, R. X., Ballmer, S., et al. 2019, in Bulletin of the American Astronomical Society, Vol. 51, 35, doi: 10.48550/arXiv.1907.04833

Remillard, R. A., & McClintock, J. E. 2006, ARA&A, 44, 49, doi: 10.1146/annurev.astro.44.051905.092532

Robson, T., Cornish, N. J., & Liu, C. 2019, Classical and Quantum Gravity, 36, 105011, doi: 10.1088/1361-6382/ab1101

Smith, K. L., Magno, M., & Tripathi, A. 2023, ApJ, 956, 3, doi: 10.3847/1538-4357/acf4f8

The LIGO Scientific collaboration. 2019, arXiv e-prints, arXiv:1904.03187, doi: 10.48550/arXiv.1904.03187

The LIGO Scientific Collaboration, the Virgo Collaboration, the KAGRA Collaboration, Abbott, R., & et al. 2021, arXiv e-prints, arXiv:2111.03606, doi: 10.48550/arXiv.2111.03606

Tremaine, S., Gebhardt, K., Bender, R., et al. 2002, ApJ, 574, 740, doi: 10.1086/341002

Virtanen, P., Gommers, R., Oliphant, T. E., et al. 2020, Nature Methods, 17, 261, doi: 10.1038/s41592-019-0686-2

Whalen, D. J., & Fryer, C. L. 2012, ApJL, 756, L19, doi: 10.1088/2041-8205/756/1/L19

Woosley, S. E. 2017, ApJ, 836, 244, doi: 10.3847/1538-4357/836/2/244